



The efficacy of an edible bird's nest in the restoration and enhancement of kidney glomeruli and peritubular capillaries in induced diabetic rats by increasing TGF- β and CD 31

Manaras Komolkriengkrai¹, Udomlak Matsathit², Rawipa Jangchart³, Nualpun Sirinupong⁴, Nisaudah Radenahmad¹, and Wipapan Khimmaktong¹

¹Department of Anatomy, Division of Health and Applied Sciences, Faculty of Science, Prince of Songkla University, Songkhla, 90110 Thailand; ²Department of Food Science and Nutrition, Faculty of Science and Technology, Prince of Songkla University, Pattani, 94000 Thailand; ³Department of Biochemistry, Division of Health and Applied Sciences, Faculty of Science, Prince of Songkla University, Songkhla, 90110 Thailand; ⁴Faculty of Agro-Industry, Prince of Songkla University, Songkhla, 90110 Thailand

*Corresponding Author: PhD, Associate Professor, Khimmaktong, W., Department of Anatomy, Faculty of Science, Prince of Songkla University, 15 Kanjanawanich Rd., Hat Yai, Songkhla, 90110 Thailand

Submission Date: March 24th, 2025, Acceptance Date: May 5th, 2025, Publication Date: May 8th, 2025

Please cite this article as: Komolkriengkrai M., Matsathi U., Jangchart R., Sirinupong N., Radenahmad N., Khimmaktong W. The efficacy of an edible bird's nest in the restoration and enhancement of kidney glomeruli and peritubular capillaries in induced diabetic rats by increasing TGF- β and CD 31. *Functional Foods in Health and Disease* 2025; 15(5): 241-256.

DOI: <https://doi.org/10.31989/ffhd.v15i5.1591>

ABSTRACT

Background: Diabetic nephropathy (DN) is primarily caused by hyperglycemia-induced angiogenesis and fibrosis. It has been reported that edible bird's nest (EDB), a traditional Chinese medicine, may prevent insulin resistance. However, its influence on diabetic nephropathy remains unclear. This research investigated the impact of EDB on diabetic nephropathy of glomeruli and peritubular capillaries in induced diabetic rat models.

Methods: Wistar rats were injected with streptozotocin (STZ) to induce diabetes mellitus (DM). Diabetic rodents were treated with EDB at doses of 75 mg/kg (EDB75), 150 mg/kg (EDB150), and glibenclamide (4 mg/kg BW) over an eight-week duration.

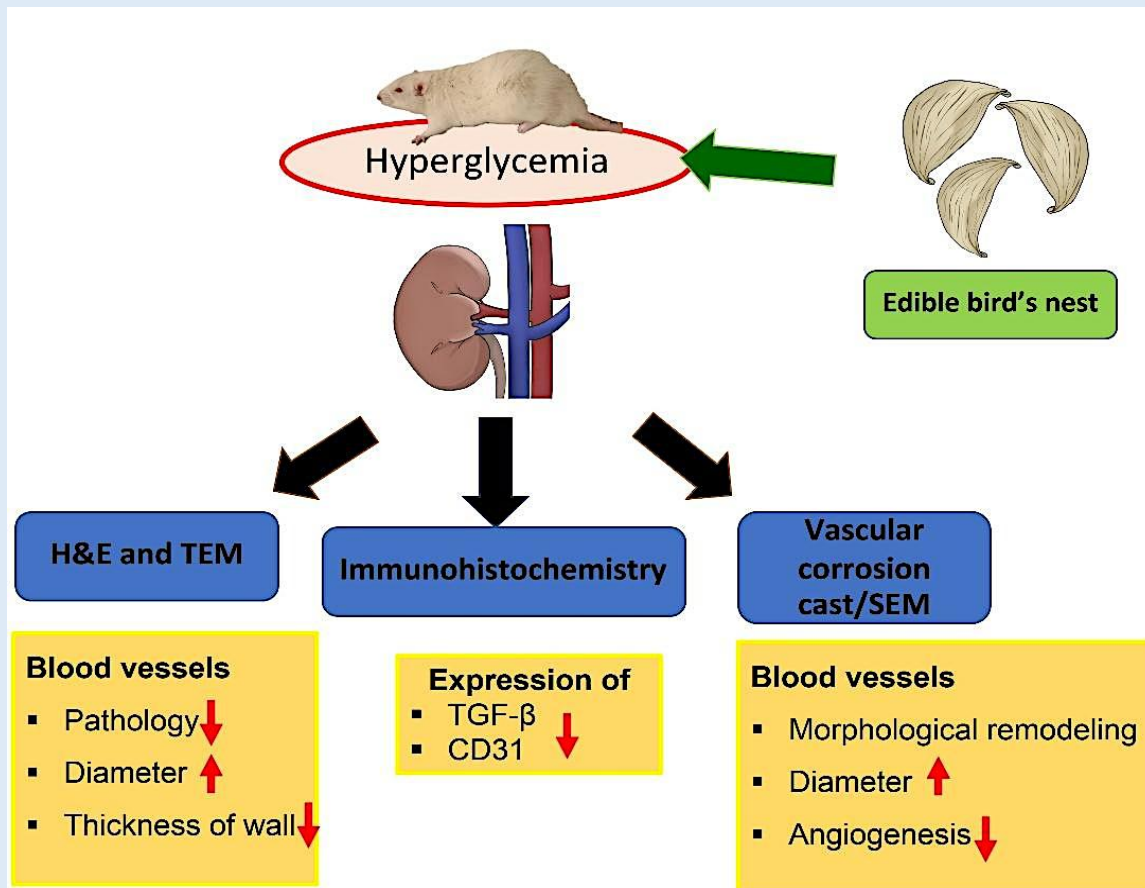
Results: The EDB 150 intervention group exhibited a decrease in fasting blood glucose levels. A histological study concluded that EDB reduced DN by reducing collagen fibers in the glomerulus while thickening the renal tubular wall. According to immunohistochemistry, EDB alleviates aberrant angiogenesis and fibrosis by decreasing the expression of

platelet-endothelial cell adhesion molecule (CD31) in endothelial cells. EDB also transforms growth factor beta (TGF- β) in glomerular and peritubular capillaries. TEM micrographs thicken the peritubular capillary and proximal tubule wall. Furthermore, the renal capillaries increased in diameter and wall thickness.

Conclusions: The current study demonstrated the potential of EDB to reduce diabetic complications. It also indicated that edible bird's nests are a potential medicinal herb for treating diabetes and kidney complications.

Novelty of the study: This study uniquely investigates the effect of edible bird's nest (EDB) on diabetic nephropathy in rat models, demonstrating its potential to reduce hyperglycemia, mitigate glomerular collagen accumulation, improve renal tubular wall thickening, and modulate aberrant angiogenesis or fibrosis by decreasing CD31 and TGF- β expression in renal tissues. These findings support the use of EDB among individuals with diabetic kidney damage.

Key words: Diabetes, kidney, Edible bird's nest, CD31, TGF- β , rat, Kidney glomeruli, Peritubular capillaries



Graphical Abstract: The efficacy of an edible bird's nest in the restoration and enhancement of kidney glomeruli and peritubular capillaries

INTRODUCTION

Diabetes mellitus (DM) is a prevalent chronic condition that results in adverse health outcomes and elevated healthcare expenses (1). The global prevalence of diabetes was 463 million in 2021 and is anticipated to rise to 578 million in 2030 and 700 million in 2045 (2). DM is a metabolic disorder distinguished by chronic hyperglycemia due to inadequate insulin secretion and function. DM may influence macrovascular and microvascular complications. Neuropathy, retinopathy, and nephropathy are microvascular complications of the condition (3). Diabetic nephropathy is used to describe renal damage that results from hyperglycemia. Diabetic nephropathy is a severe complication of the disease. Complications begin with glomerular hypertrophy and hyperfiltration, which is followed by the thickening of tubular and Bowman's capsule basement membranes, and the expansion of the mesangial matrix (4). End-stage renal disease results in long-term diabetic nephropathy, contributing to a decline in renal function.

The progression of diabetic nephropathy is characterized by an increase in extracellular matrix production, angiogenesis, and endothelial cell proliferation (5). Vascular endothelial growth factor (VEGF) contributes to the proliferation and angiogenesis of endothelial cells. Furthermore, hyperglycemia leads to an increased production of reactive oxygen species. The endothelium expresses CD 31, a transmembrane glycoprotein. Angiogenesis is indicated by CD31 (6). Abnormal angiogenesis results from elevated VEGF and ROS levels in diabetic nephropathy, which impacts the glomerular filtration rate. (7). Mesangial expansion is another consequence of diabetic neuropathy due to the accumulation of extracellular matrix in the glomerulus and the aberrant proliferation of mesangial cells (8). The accumulation of extracellular matrix, which is induced by hyperglycemia, is facilitated by transforming growth factor-beta (TGF- β). Additionally, hyperglycemia induces

glomerular dysfunction and glomerulosclerosis due to elevated VEGF and TGF- β levels (9).

Current treatment options for diabetic nephropathy are challenging and costly. Swiftlets in Southeast Asia generate edible bird's nest (EDB), a valuable animal bioproduct. EDB has been employed as a traditional Chinese medicine that improves energy and health (10). EDB provides significant antioxidant and anti-inflammatory effects (11). In addition, EDB demonstrated a protective effect against hyperglycemia by enhancing β -cell function and insulin signaling by alleviating oxidative stress-induced chronic inflammation in diabetic rat models (12). However, the impact of edible bird's nest on diabetic nephropathy remains uncertain. This investigation aims to determine the effects of edible bird's nest on diabetic nephropathy in diabetic rat models by analyzing morphological changes and protein expression of cluster of differentiation 31 (CD31) in the kidney.

MATERIALS AND METHODS

Preparation of EBN extract: Nakhon Si Thammarat, Thailand, supplied the edible bird's nest (EBN) that had been cleansed and dried. To obtain EBN water extract powder, the EBN extract preparation was conducted with a minor modification from Careena (13) and Yew (14). Using a dry grinding mill, the EBN was weighed and pulverized into a fine powder. The material was dissolved in distilled water at a ratio of 1:40 (w/v) at 4°C for 24 hours. The softened EBN was subsequently placed in a stewing vessel and cooked at 95–98°C for 8–9 hours, or until it was fully molten. The solution was gently stirred with a magnetic agitator during the stewing process. The homogeneous solution was subsequently lyophilized using a freeze-dryer after cooling. The resulting EBN extract powder was aliquoted and stored at -20°C for use in subsequent experiments.

Animals: Wistar rats (8 weeks old, 200-250 g) were purchased from Nomura Siam International Co., Ltd. Animals were acclimated to the laboratory environment for 7 days. Animals were housed under standard laboratory conditions under a 12-hour light/dark cycle, with a moderate temperature (25±2°C). The lights were turned on at 7:00 a.m., while humidity (50±10%) and ventilation were maintained to provide a hygienic environment. The rats were fed ad libitum and standard rat chow containing protein, carbohydrates, fat, vitamins, and minerals. This study followed the guidelines provided by the Animal Ethics Committee of the Prince of Songkhla University.

Rats were randomly divided into control groups and a diabetic group. The control group (C) was injected intravenously with 0.1 mol/l citrate buffer into the lateral tail vein. The diabetic group was injected intraperitoneally with a single 60 mg/kg dose of streptozotocin (STZ; Sigma-Aldrich; Merck KGaA) dissolved in 0.1 mol/l citrate buffer (pH 4.5) (Sigma-Aldrich; Merck KGaA). Three days after the injection, blood glucose levels were measured using an Accu-Chek Active® one-touch glucometer and test strips (Roche Diagnostics GmbH). The rats with a blood glucose level ≥ 250 mg/dl were considered diabetic. The diabetic rats were divided into 3 groups (10 animals each). The first group (EDB 75) received EDB 75 mg/kg, the second group (EDB 150) received EDB 150 mg/kg, and the last one (GR) received glibenclamide (4 mg/kg BW) in 0.5 ml 0.5% Tween-80 solutions. Each group was fed a balanced, standard diet throughout the study.

Each animal was weighed and had blood glucose levels measured once per week. After the final administration, rats were euthanized with an excessive dose of Thiopental (150 mg/kg; intraperitoneal injection). Following the animal sacrifice, the kidney of each model was collected. Half of the rats in each group were used to

examine H&E and immunohistochemistry staining using bodily tissues. The other half of the rats in each group were injected with resin to promote vascular corrosion, casting combined scanning electron microscopy (15).

Histological preparation for Masson's trichrome

staining: The kidney was fixed and embedded in paraffin to analyze any histological changes of the glomerulus in kidney tissue from all groups. Kidney tissues embedded in paraffin were cut into 5-µm-thick sections and stained at room temperature with a Masson trichrome (Trichrome Stain (Masson) kit, HT15, Sigma-Aldrich; Merck KGaA). This staining technique is commonly used to detect collagen fibers (16) in the glomerulus of the kidney. All sections were observed and evaluated under an Olympus BX50 light microscope using an Olympus DP73 camera (Olympus Corporation; magnification, x600). The lumen diameter of the arteries was measured using CellSens software (v1.16, Olympus Corporation).

Immunofluorescence study: The cut kidney tissues were deparaffinized in xylene, hydrated through a descending series of ethanol to distilled water, and permeabilized in PBS with 0.1% Triton X-100 (PBST) for 30 minutes to analyze TGF-β levels. The rabbit monoclonal anti-TGF-β (Abcam, Cambridge, UK) was diluted 1:200 in the blocking serum. Then, the product was incubated at 4°C overnight after blocking was performed, using equine serum in PBS for 1 hour at room temperature. To detect TGF-β, the sections were exposed to Texas red goat anti-rabbit IgG (H+L) antibody (1:200; Vector Laboratories, Inc.) in blocking solution for 2 hours at room temperature in the dark, following three washes with PBS. The images were analyzed using a fluorescence microscope (BX-50, Olympus Corporation). The fluorescence intensity was measured using National Institutes of Health (NIH) Image J software 1.52, which was used to ascertain the TGF-β percentages of cell expression.

Immunohistochemistry: Immunohistochemistry staining detects CD31, an endothelial cell marker. Kidney tissues embedded in paraffin were cut into 5 μm . The paraffin sections were deparaffinized in xylene. The slides were then permeabilized in PBS with 0.1% Triton X-100 (PBST) for 30 minutes. The blocking process was performed using horse serum in PBS for 1 hour at room temperature, followed by incubation with anti-CD31 antibody at 4°C overnight. The sections were exposed to the secondary antibody in the blocking solution for 2 hours to detect CD31 at room temperature. Images were examined and photographed under a microscope (Olympus D73 equipped with CellSens software).

Vascular corrosion casting technique/SEM: Vascular corrosion casting was performed using an intravascular injection of 0.9% standard saline solution (General Hospital Products Public Co., Ltd.) to remove blood from the vascular bed. Subsequently, Batson No. 17 immediately injected the plastic mixture into the cannula through the ascending aorta until retraction from the venous vessels became evident. The plastic mix was immediately injected into the cannula through the ascending aorta until a reflux from the venous vessels became evident. The kidney was cut and immersed in water at 80 °C to complete the hardening process. Then, the kidney underwent a corrosive process by adding a 10% potassium hydroxide (KOH) solution (Vidhyasom Co., Ltd.) at room temperature for 1 month. Tissues were removed and washed with distilled water. The kidney vascular cast was dissected into small specimens and air-dried for 2 weeks. The vascular cast of the kidney was placed on a metal stub with double-sided adhesive tape, sprayed with carbon paint, and coated with gold on a sputtering apparatus before preparation for scanning electron microscopy observation (JEOL JSM-5400; JEOL, Ltd.) at 10-15 kV. The diameters of afferent arterioles,

efferent arterioles, glomeruli, and peritubular capillaries were measured using SemAfore 5.2 software (JEOL, Ltd.).

Transmission electron microscopy technique: The kidneys were cut into small cubes of 1 × 1 × 1 mm. The samples were fixed with primary fixation (2.5% glutaraldehyde + 4% formaldehyde in 0.1M PBS) for 2 hours and then washed with 0.1M PBS for 5 minutes, 3 times. Then, the kidneys were dehydrated in ethyl alcohol and infiltrated with propylene oxide (PO) 2 times for 30 minutes and then incubated in PO: Araldite 502 resin (2:1) for 1 hour and (1:2) for 12–14 hours. Kidneys were embedded in pure Araldite 502 resin polymerized for 24 hours at 40 °C and 48 hours at 60 °C, respectively. Kidneys were then cut into ultra-thin sections (60-90 μm) using an ultramicrotome. The sections were then placed on a copper grid and stained with saturated uranyl acetate in a 70% methanol and 0.1% lead citrate solution in water for 15. Sections were observed with a transmission electron microscope.

Statistical analysis: The data are presented as means \pm standard error of the mean. Statistical analysis was conducted using ANOVA and the Bonferroni post hoc test. A P-value of less than 0.05 indicated a statistically significant difference.

RESULTS

Effects of EDB on Fasting blood glucose (FBG) levels and body weight in diabetic rats: The FBG levels are noted in Figure 1. FBG levels significantly increased in the DM group compared to the C group ($p < 0.01$). There was a significant decrease by EDB and glibenclamide administration (Figure 1). The DM group's body weight was reduced considerably compared to the control group. After treatment with EDB and glibenclamide, the results significantly improved compared to the DM group ($p < 0.01$).

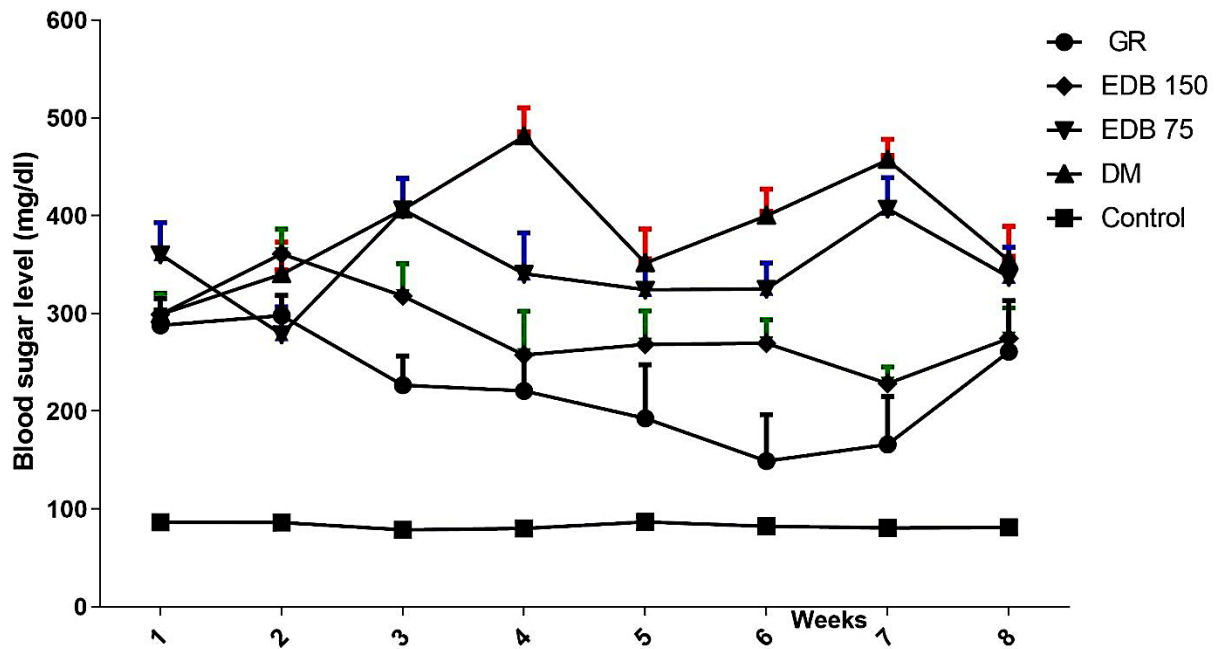


Figure 1: Fasting blood glucose levels in different groups

Effects of EDB on Blood Urea Nitrogen (BUN) and Creatinine (Cr) levels in diabetic rats: Blood urea nitrogen and creatinine levels were measured to assess kidney function. BUN level of the DM group significantly increased when compared with the control group ($p <$

0.001). After treatment with EDB and glibenclamide, BUN levels decreased, but did not show significance. Creatinine levels also showed no significant difference in each group (Figure 2).

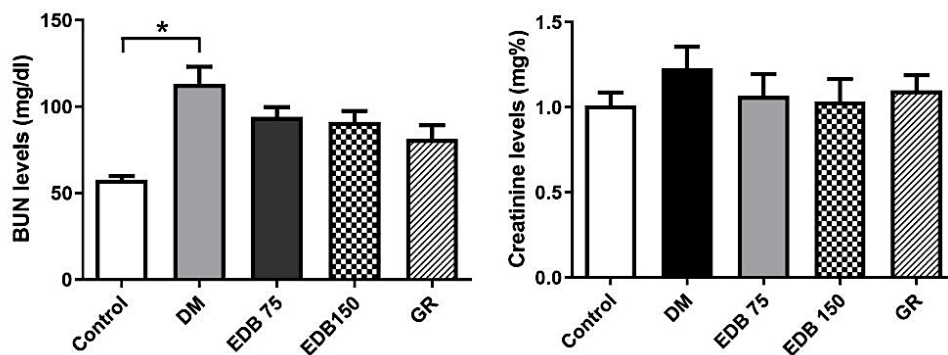


Figure 2: Blood Urea Nitrogen and Creatinine levels in different groups. * $p < 0.001$ compared with the control group

Effects of EDB on Masson's trichome histological observation in diabetic rats: The histology of the control group displayed a normal glomerulus. Masson's trichrome staining shows the accumulation of collagen fibers around mesangial cells, which causes mesangial

cell matrix expansion in the glomerulus of the DM and EDB 75 groups. After 8 weeks of treatment with EDB 150 and glibenclamide, collagen fiber accumulation was reduced significantly (Figure 3).

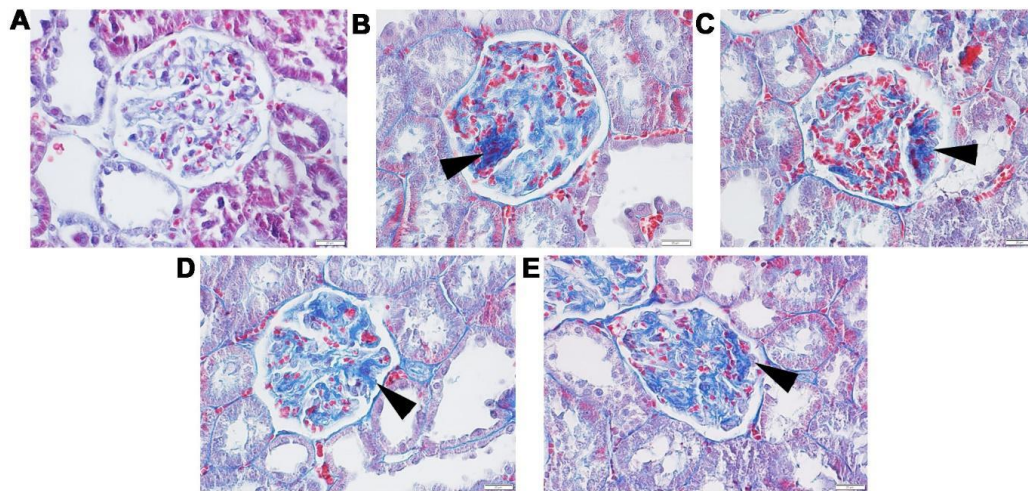


Figure 3 Photomicrographs of Masson's trichrome staining show the histological structure of the glomerulus in Control (A), DM (B), EDB 75 (C), EDB 150 (D), and GR (E) rats. Black arrows indicated the accumulation of collagen fibers. Scale bar = 20 μ m.

Effects of EDB on the expression levels of TGF- β in diabetic rats' glomeruli and peritubular capillaries:

Immunofluorescent reactions that transform growth factor beta (TGF- β) protein in kidney tissues were stained fluorescent red in the smooth muscle layer and the internal elastic lamina of the vessel wall (Figure 4). The study of TGF- β expression in the kidneys of each group of rats showed: Controls (30.82 ± 0.633), DM (44.67 ± 0.89),

EDB75 (39.87 ± 1.91), EDB150 (34.38 ± 0.98), and GR (31.56 ± 0.87). Therefore, rats in the DM group had significantly increased TGF- β expression ($p < 0.0001$) compared to the control group. When treated with the bird's nest extract in the EDB75 and EDB150 groups, and glibenclamide in the GR group, the expression of TGF- β decreased significantly in EDB150 ($p < 0.05$) and GR ($p < 0.001$) when compared to the DM group (Figure 5).

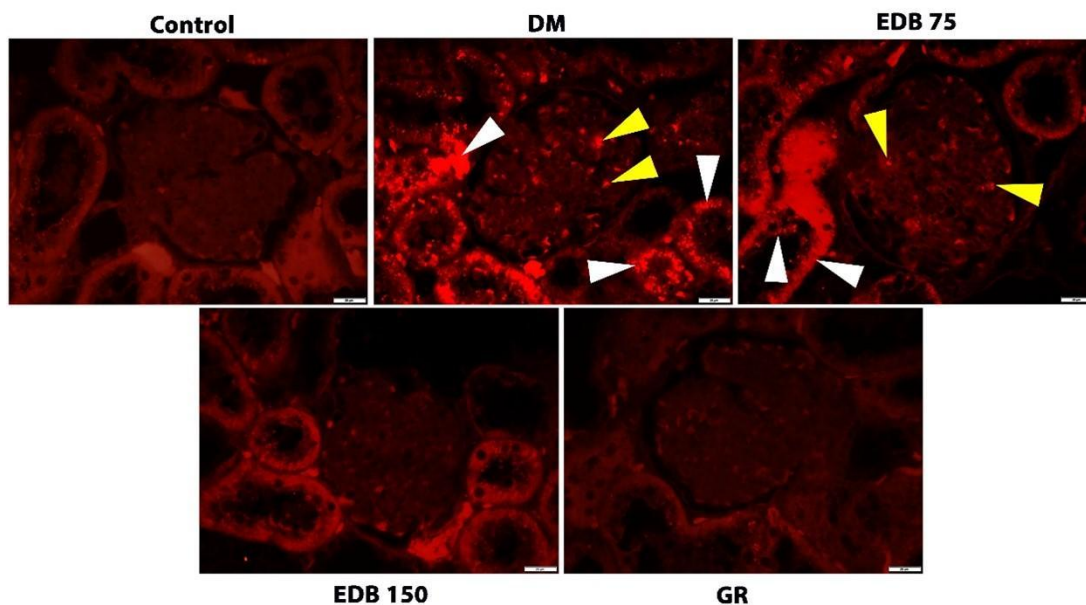


Figure 4. The expression of TGF- β in glomeruli and peritubular capillaries was determined by immunofluorescence. Control (A), DM (B), EDB 75 (C), EDB 150 (D), and GR (E). The staining outcomes were observed under a microscope. White arrows indicated the positive staining area of TGF- β in the peritubular capillaries. Yellow arrows indicate the positive staining area of TGF- β in the glomerulus. Scale bar = 20 μ m

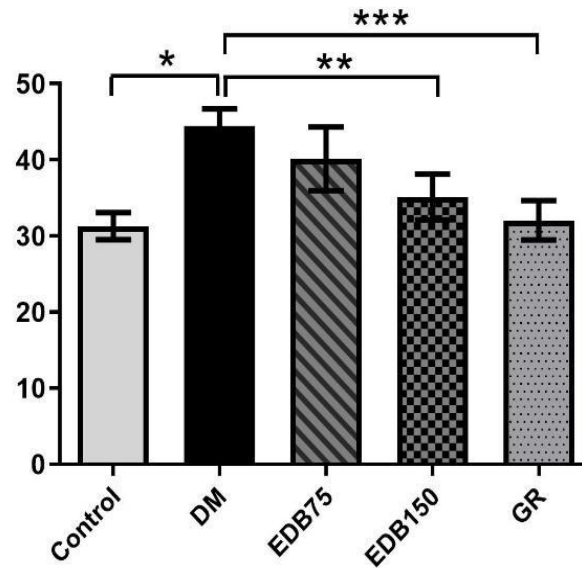


Figure 5: Optical density of TGF-β in glomeruli and peritubular capillaries of each group. (*) $p < 0.0001$ was significantly different compared with the control group. (**) $p < 0.05$, (***) $p < 0.001$ significantly differed from the DM group.

Effects of EDB on the expression levels of CD-31 in diabetic rats’ glomeruli and peritubular capillaries: The expression of CD-31 in the glomerulus (Figure 6) and peritubular capillary (Figure 7) was evaluated through immunohistochemistry staining. As shown in Figures 5 and 6, the results found that the expression of CD31 in

endothelial cells of glomerular and peritubular capillaries significantly increased in the DM group ($p < 0.001$) compared to the controls. After treatment, the expression of CD31 significantly decreased in the EDB150 and glibenclamide groups compared with the DM group ($p < 0.01$) (Figure 8).

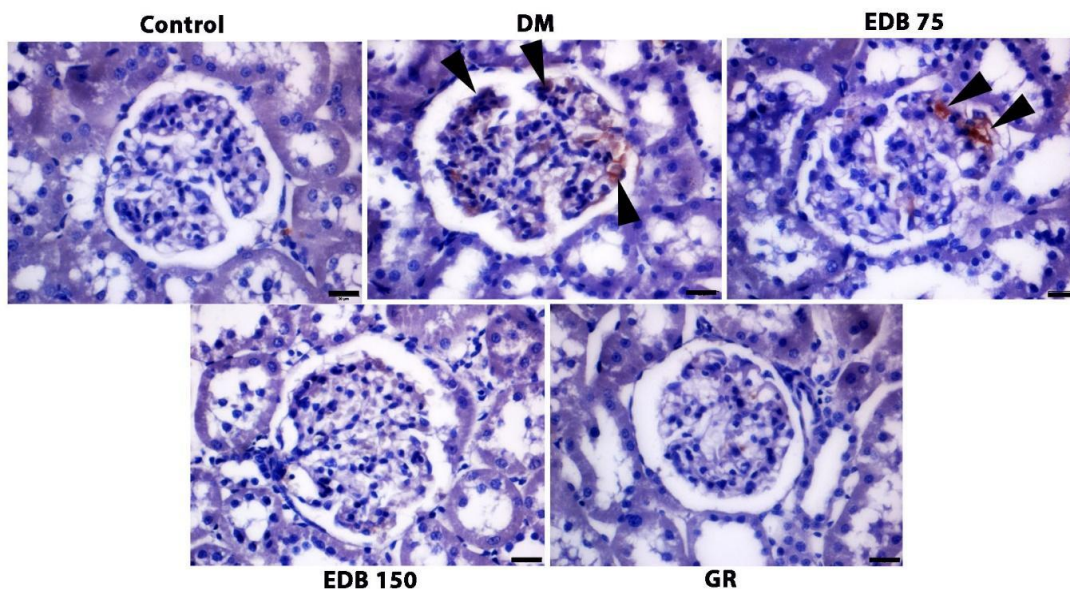


Figure 6. The expression of CD31 in glomeruli was determined by immunohistochemistry. Control (A), DM (B), EDB 75 (C), EDB 150 (D), and GR (E). The staining outcomes were observed under a microscope. The black arrow indicates the positive staining area of CD 31. Scale bar = 20 μm

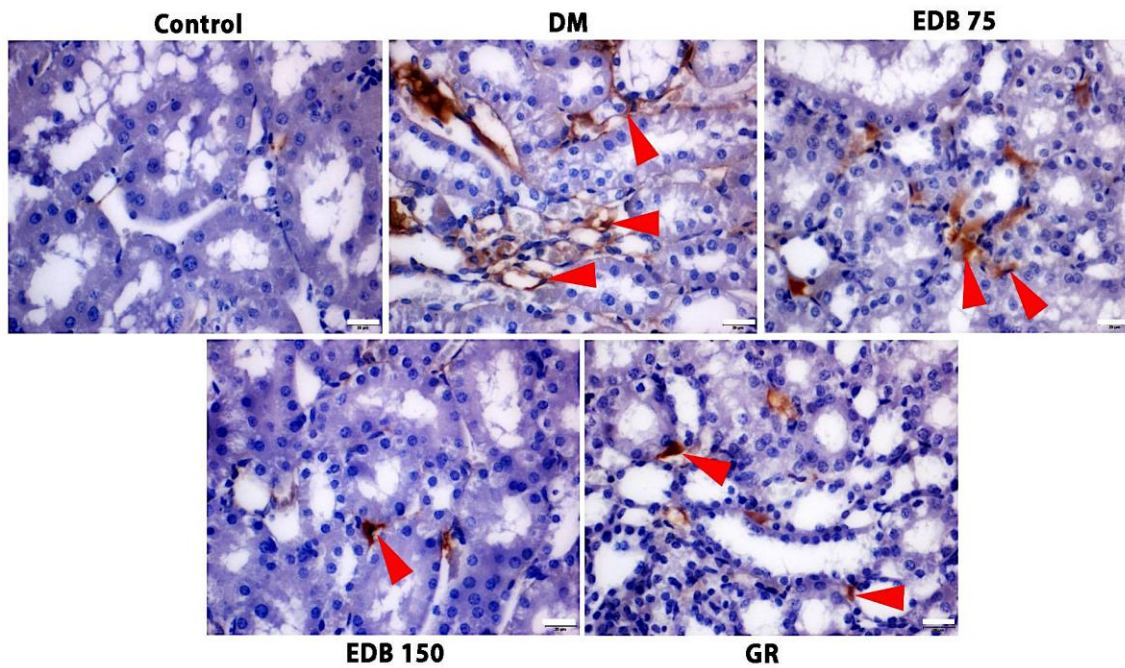


Figure 7. The expression of CD31 in peritubular capillaries was determined by immunohistochemistry. Control (A), DM (B), EDB 75 (C), EDB 150 (D, and GR (E). The staining outcomes were observed under a microscope. The red arrow indicates the positive staining area of CD 31. Scale bar = 20 μm.

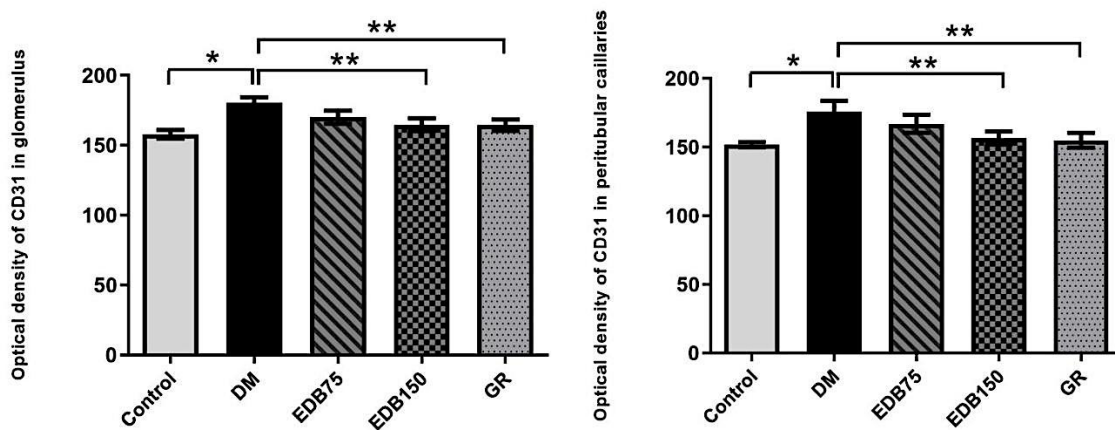


Figure 8: Optical density of CD 31 in glomeruli and peritubular capillaries of each group. (*) $p < 0.001$ was significantly different compared with the control group. (**) $p < 0.001$ was significantly different compared with the DM group.

Vascular corrosion cast examination: The stereomicroscope was utilized to evaluate the vascular corrosion casts of kidneys in the control, DM, EDB75, EDB150, and GR groups at low magnification. In the control group, the renal artery, including afferent and efferent arterioles, peritubular capillaries, and glomerulus, was of normal size and had no diminution (Figure 9A). However, the DM and EDB 75 groups exhibited a reduced vascular density in the cortex and

medulla, with blood vessels disintegrating (Figure 9B, 9C). Additionally, the glomerulus was damaged. The glomerulus exhibited fragmentation and contraction in certain capillaries. Following treatment with EDB150 (Figure 9D) and glibenclamide (Figure 9E), the nephron's blood vessel supply and dimensions of afferent and efferent arterioles, peritubular capillaries, and glomerulus were enhanced in the DM group.

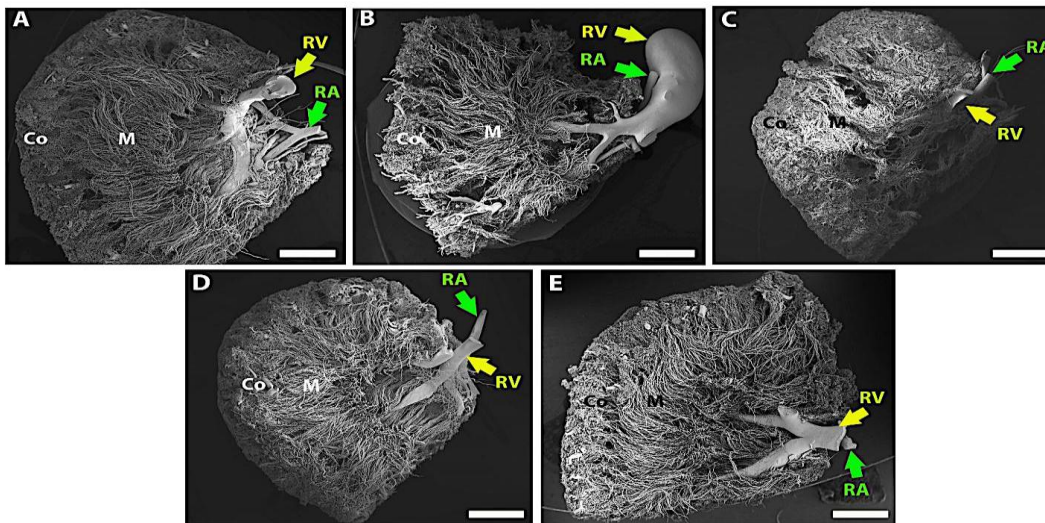


Figure 9 Vascular corrosion casts of the kidney of Wistar rats. Low magnification scanning electron micrograph of half of the kidney showed renal cortex (Co), renal medulla (M), Renal artery (RA), and Renal vein (RV). Control (A), DM (B), EDB 75 (C), EDB 150 (D, and GR (E). (Scale bar = 1 mm)

In the DM group, the size of the glomerulus shrank, but did not show any significance compared to the control group. Additionally, results from the EDB75, EDB150, and GR groups revealed a rise in glomerulus size, which was not significantly higher than those with DM (Figure 10B). Afferent arteriole diameters significantly decreased in the DM group compared to the controls (Figure 10A). After treatment with EDB75 (Figure 10C), EDB150 (Figure 10D), and glibenclamide (Figure 10E), the

results showed significant increases in diameter for both EDB150 and glibenclamide. Still, they showed no significant increase in EDB75 compared to the DM group. The diameters of the efferent arterioles and peritubular capillaries in the DM group decreased significantly compared to the control group. However, no significant differences were observed in the EDB75, EDB150, and GR groups (Table 1).

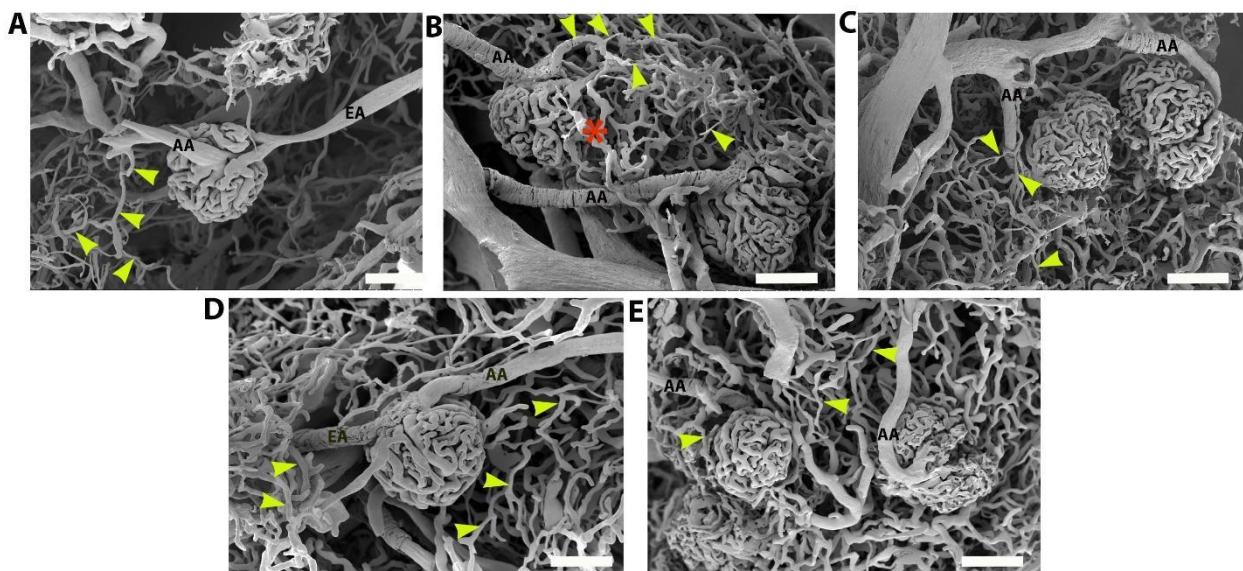


Figure 10 Low magnification scanning electron micrograph of the glomerulus and peritubular capillaries in Control (A), DM (B), EDB 75 (C), EDB 150 (D, and GR (E). Yellow arrows indicated peritubular capillaries. Efferent arteriole (EA), afferent arteriole (AA), * demonstrated vessel damage. (Scale bar = 50 μm)

Table 1: Data showed the diameter of afferent arterioles, efferent arterioles, glomeruli, and peritubular capillaries in five groups of animals.

Groups	Diameter of Afferent arterioles (µm)	Diameter of Efferent arterioles (µm)	Diameter of glomeruli (µm)	Diameter of Peritubular capillaries (µm)
Control	16.71±0.55	12.24±0.74	111.65±2.68	7.41±0.93
DM	10.52±1.44*	8.40±0.76*	104.83±9.71	5.29±0.21
EDB75	11.29±1.50*	9.10±0.88*	107.43±7.48	5.47±0.43
EDB150	14.22±0.65**	10.18±0.11	113.28±5.88	7.05±0.81
GR	15.98±0.90**	11.26±0.38	114.80±4.50	7.57±0.31

(*) $p < 0.01$ was significantly different compared with the Control group. (**) $p < 0.05$ was significantly different compared with the DM group.

Transmission Electron micrograph of peritubular capillary:

Peritubular capillaries are blood capillaries surrounding the cortical nephrons' PCT and DCT, as shown in Figure 11A. In DM (Figure 11B) and EDB 75 (Figure 11C) groups, peritubular capillaries experienced thickening and multilayer basement membrane formation or thickening between peritubular capillaries and proximal tubule walls. Red blood cells and platelets

accumulated in the lumen of peritubular capillaries (Figure 11B). The proximal tubule displayed swollen mitochondria. However, treatment with EDB150 (Figure 11D) and GR (Figure 11E) was concluded to improve thickening and multilayer basement membrane formation between the peritubular capillary and the proximal tubule wall.

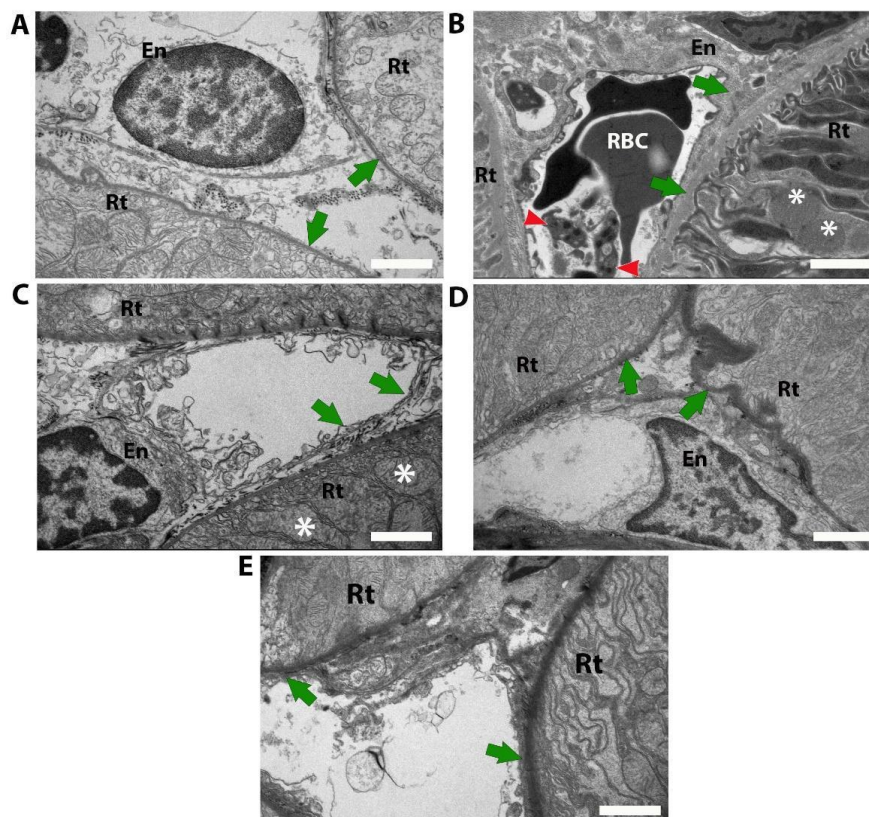


Figure 11 Transmission Electron micrograph of a Peritubular capillary (PC) located between the proximal tubule (T) wall. Black arrows indicated the basement membrane of endothelial cells (En) of the peritubular capillary, and black arrowheads indicated platelet cells. The proximal tubule shows the swollen mitochondria (white asterisks). Control (A), DM (B), EDB 75 (C), EDB 150 (D), and GR (E). (Scale bar = 2 µm)

DISCUSSION

This study investigated the effect of edible bird's nest on DM rats after 8 weeks of treatment. The EDB rats were found to have significantly lower weight and serum glucose levels than the DM group. According to EDB, reduced serum glucose levels in DM rats (12) are due to decreased reactive oxygen species markers such as NOX-2 and nitrotyrosine and increased antioxidants such as SOD-1 and phosphorylated eNOS in endothelial cells (16). In addition, EDB improved renal function parameters, including creatinine (Cr) and blood urea nitrogen (BUN), in diabetic rats.

Hyperglycemia elevates the production of oxidative stress. Hyperglycemia creates an optimal environment for free radicals. Advanced glycosylated end-products (AGEs) are generated when glucose forms a bond with the proteins in cells (non-enzymatic glycation) (17). In addition, the binding of AGEs to their receptors in vascular permeability and free radicals, causing a thickened basement membrane and an increase in collagen types 1 and 4. This decreases the elasticity of blood vessels, which affects the function of eNOS and guanylyl cyclase (18). This leads to a reduced vascular response to nitric oxide (NO), primarily due to the increased formation of free radicals through enzyme-independent and enzyme-dependent mechanisms. Enzyme-dependent mechanisms activate protein kinase C (PKC), a protein involved in intracellular signaling, stimulated by diacylglycerol (DAG), which is produced from glycolysis in hyperglycemia. This activates PKC- β , which promotes the expression of vascular endothelial growth factor (VEGF) and transforms growth factor-beta (TGF- β). Thus, bird's nest aids in the reduction of NO levels and ROS generated from NADPH oxidase, resulting in vascular endothelial dysfunction in diabetes patients (12). The receptor is bound by the accumulation of advanced glycosylated end-products (AGEs) (19). AGEs induce endothelial dysfunction by increasing vascular permeability (20), thickening the basement membrane,

and reducing the elastic properties of blood vessels through an increase in collagen types 1 and 4 (21, 22). Additionally, hyperglycemia induced an increase in diacylglycerol (DAG), which increased the activity of protein kinase C (PKC) associated with vascular endothelial growth factor (VEGF) and transforming growth factor-beta (TGF- β) (23, 24). VEGF influences abnormal angiogenesis. CD 31 is an angiogenic marker elevated in diabetic rodents (25). The expression of CD31 in diabetic rodents decreased following treatment with EDB. Intriguingly, EDB can potentially treat DM by reducing vascular endothelial dysfunction and aberrant angiogenesis.

The most abundant membrane glycoprotein constitutively expressed on the vascular endothelium is CD31, a highly glycosylated Ig-like membrane receptor expressed by leukocytes, platelets, and endothelial cells. CD31 may contribute to the accumulation of leukocytes within atherosclerotic plaques. However, its precise function is unclear (26). The vascular endothelium's physiological functions are maintained by the dense presence of CD31 on its surface (27). In this context, it facilitates signaling essential for the cytoprotection and barrier function of the adjacent endothelial cells, while increasing the activation threshold of blood-flowing platelets and leukocytes. This is done by engaging in transhomophilic interactions with their respective CD31 molecules (28). The dense presence of CD31 on its surface maintains the vascular endothelium's physiological functions.

This study evaluated the morphological change in afferent arterioles, efferent arterioles, and peritubular capillaries. Peritubular capillaries are tiny blood vessels located inside the kidneys. These blood vessels work alongside nephrons, which are filtering units, to rid the body of excess water and waste. After passing through the peritubular capillaries and nephrons, waste is turned into urine that travels to the bladder and exits the body. Peritubular capillaries help the body reabsorb nutrients

and excrete waste. Thickening the basement membrane hinders the efficient exchange of oxygen, nutrients, and waste products between the peritubular capillaries and renal tubules. The DM group showed the thickening of peritubular capillaries in the basement membrane. This thickening is due to chronic hyperglycemia, leading to the accumulation of advanced glycation end-products (AGEs) and an increased synthesis of extracellular matrix proteins. The thickening of the walls of blood vessels reduces vascular flow and blood supply to the kidney. Peritubular capillary basement membrane thickening disrupts normal renal microvascular and tubular function, which contributes to hypoxia, fibrosis, and progressive kidney damage. However, treatment with EDB improved the diameter of blood vessels compared to the DM group.

The study of histological change showed that the glomeruli were damaged from hyperglycemia. Glomerular hypertrophy was found in the diabetes group. This is caused by hyperglycemia-inducing glomerular capillary injury, which results in more rapid cell division within the glomerulus (29). In addition, hyperglycemia stimulates mesangial cells, cells within the glomerulus, to synthesize extracellular matrix (30). The accumulation of extracellular matrix causes the enlargement of the glomerulus. Yet, when diabetic rats were treated with 150 mg of EDB and glibenclamide, the improvement in glomerulus was comparable to the control group. Diabetic nephropathy is the thickening of the basement membrane in peritubular capillaries and the walls of the proximal tubules in the kidney. High TGF- β levels cause this. The thickening of the basement membrane in peritubular capillaries and the proximal tubule walls in the kidney is due to increased TGF- β levels. This is a hallmark of diabetic nephropathy, which is driven by hyperglycemia-induced activation of various signaling pathways and subsequent overproduction of extracellular matrix (ECM) components. Here's how TGF- β mediates this effect. TGF- β induces endothelial-to-

mesenchymal transition (EndMT) in peritubular capillary endothelial cells, causing them to lose their endothelial characteristics (e.g., CD31 expression) and gain mesenchymal traits, such as ECM production. This leads to excessive collagen deposition and thickening of the capillary basement membrane, impairing capillary permeability and nutrient exchange.

Hyperglycemia increases the endothelial nitric oxide synthase (eNOS). eNOS plays a significant role in endothelial functions. It also stimulates the production of nitric oxide (NO). When NO and superoxide were elevated, that stimulated peroxynitrite production (31). The increase in peroxynitrite and other oxidative stressors induces the inflammation of endothelial cells and causes endothelial cell dysfunction (32). When endothelial cells were damaged by inflammation, the healing processes were stimulated by transforming growth factor beta (TGF- β). TGF- β stimulated collagen production (33). The accumulation of collagen at the basement membrane of endothelial cells leads to the thickening of arterial walls. TGF- β drives the thickening of the basement membrane in peritubular capillaries and proximal tubules by upregulating ECM protein synthesis, reducing ECM degradation, and promoting pathological cellular transitions like EMT and endothelial-to-mesenchymal transition (EndMT) (34). These processes lead to structural and functional renal impairment, central to diabetic nephropathy progression.

TGF- β (Transforming Growth Factor Beta) and CD31 (also known as PECAM-1 or Platelet Endothelial Cell Adhesion Molecule-1) are involved in processes significant in diabetes-related complications, particularly those associated with hyperglycemia. Their connection can be understood in the context of vascular dysfunction, inflammation, and tissue remodeling, which is common in diabetic pathophysiology. TGF- β is a cytokine that plays a central role in tissue remodeling, fibrosis, and inflammation. In diabetes, hyperglycemia can upregulate the expression of TGF- β , contributing to complications

such as diabetic nephropathy, retinopathy, and cardiovascular disease. TGF- β promotes extracellular matrix deposition, leading to fibrosis in tissues such as the kidney and blood vessels. It also has immunomodulatory effects, influencing macrophage activation and inflammatory responses. CD31 is a glycoprotein predominantly expressed on endothelial cells and is crucial for maintaining vascular integrity and endothelial cell-cell interactions. It has anti-inflammatory and anti-apoptotic properties, supporting vascular health. In diabetes, hyperglycemia and oxidative stress can impair CD31 function or expression, contributing to endothelial dysfunction and increased vascular permeability. In diabetic animal models, hyperglycemia induced upregulation of TGF- β , while changes in CD31 expression were observed in tissues prone to complications (e.g., kidneys, retina, and vasculature).

This research presents a significant innovation of the true therapeutic potential of edible bird's nest (EDB), a traditional Chinese medicine, in diabetic nephropathy (DN). While EDB's effects on insulin resistance have been previously reported, this study uniquely elucidates its impact on the structural and molecular hallmarks of DN, specifically demonstrating its ability to reduce hyperglycemia and attenuate angiogenesis (via CD31) and fibrosis (via TGF- β) in the kidney glomeruli and peritubular capillaries of diabetic rat models. The histological improvements and modulation of key angiogenic and fibrotic markers provide a novel scientific basis for EDB's traditional use.

The practical implications of these findings are promising for managing DN, a major complication of diabetes. EDB, as a natural product, could represent a novel or adjunctive therapeutic strategy to slow the progression of kidney damage in diabetic patients. The study's identification of EDB's effects on TGF- β and CD31 suggests potential mechanisms that align with current therapeutic targets for DN. Further research into the specific bioactive components of EDB responsible for

these effects could lead to the development of targeted therapies or dietary interventions. This study encourages the exploration of EDB as a complementary approach to conventional treatments for DN, which may offer a holistic strategy to protect kidney function in diabetic individuals.

CONCLUSIONS

This research has demonstrated that EDB reduces FBG levels. Its effects can prevent angiogenesis and decrease the accumulation of extracellular matrix. Therefore, EDB may improve and restore the pathogenesis of the glomerulus and blood vessels damaged by hyperglycemia. Therapeutic interventions targeting TGF- β signaling or preserving CD31 expression have been explored to mitigate diabetic complications. For instance, it has been reported that inhibiting TGF- β activity may reduce fibrosis, while enhancing CD31 function could improve endothelial repair and reduce inflammation.

Abbreviation: DN: Diabetic nephropathy, EDB: edible bird's nest, STZ: streptozotocin, CD31: platelet-endothelial cell adhesion molecule, TGF- β : transforming growth factor beta, TEM: transmission electron microscope, H&E: hematoxylin and eosin, KOH: potassium hydroxide, FBG: Fasting blood glucose, BUN: Blood Urea Nitrogen, Cr: creatinine.

Acknowledgments and Funding: This research was supported by the National Science, Research, and Innovation Fund (NSRF) and Prince of Songkla University (Grant No. AGR6505062M), Thailand.

Authors' contributions: WK designed and conducted the research. NS prepared the edible bird's nest. MK and RJ prepared the tissue and performed staining. WK, UM, and RJ performed the vascular corrosion cast. WK and MK performed the TEM method. WK wrote the manuscript and performed the statistical analysis. All authors read and approved the final version of the manuscript.

Competing interests: The authors declare that they have no competing interests.

REFERENCES

- Arneth B, Arneth R, Shams M. Metabolomics of type 1 and type 2 diabetes. *Int J Mol Sci.* 2019;20:2467. DOI: <https://doi.org/10.3390/ijms20092467>
- Maliwal D, Pissurlenkar RRS, Telvekar V. Identification of novel potential anti-diabetic candidates targeting human pancreatic α -amylase and human α -glycosidase: an exhaustive structure-based screening. *Can J Chem.* 2021;100:338-352. DOI: <https://doi.org/10.1139/cjc-2021-0117>
- Graves LE, Donaghue KC. Vascular complications in adolescents with diabetes mellitus. *Front Endocrinol (Lausanne).* 2020;11:370. DOI: <https://doi.org/10.3389/fendo.2020.00370>
- Tian S, Tang J, Liu H, Wang L, Shen J, Li J, et al. Propyl gallate plays a nephroprotective role in the early stage of diabetic nephropathy associated with suppression of glomerular endothelial cell proliferation and angiogenesis. *Exp Diabetes Res.* 2012;209567. DOI: <https://doi.org/10.1155/2012/209567>
- Kolset SO, Reinholt FP, Jenssen T. Diabetic nephropathy and extracellular matrix. *J Histochem Cytochem.* 2021; 60:976-986. DOI: <https://doi.org/10.1369/0022155412459994>
- Takahashi R, Tanaka S, Hiyama T, Ito M, Kitadai Y, Sumii M, et al. Hypoxia-inducible factor-1 α expression and angiogenesis in gastrointestinal stromal tumor of the stomach. *Oncol Rep.* 2003;10:797-802. DOI: <https://doi.org/10.3892/or.10.3.797>
- Zhang A, Fang H, Chen J, He L, Chen Y. Role of VEGF-A and LRG1 in abnormal angiogenesis associated with diabetic nephropathy. *Front Physiol.* 2020;11:1064. DOI: <https://doi.org/10.3389/fphys.2020.01064>
- Thomas HY, Ford Versypt AN. Pathophysiology of mesangial expansion in diabetic nephropathy: mesangial structure, glomerular biomechanics, and biochemical signaling and regulation. *J Biol Eng.* 2022;16:19. DOI: <https://doi.org/10.1186/s13036-022-00286-0>
- Nagai Y, Matoba K, Kawanami D, Takeda Y, Akamine T, Ishizawa S, et al. ROCK2 regulates TGF- β -induced expression of CTGF and profibrotic genes via NF- κ B and cytoskeleton dynamics in mesangial cells. *Am J Physiol Renal Physiol.* 2019;317:F839-F851. DOI: <https://doi.org/10.1152/ajprenal.00158.2019>
- Vimala B, Hussain H, Nazaimoon WMW. Effects of edible bird's nest on tumour necrosis factor- α secretion, nitric oxide production and cell viability of lipopolysaccharide-stimulated RAW 264.7 macrophages. *Food Agric Immunol.* 2012;23:303-314. DOI: <https://doi.org/10.1080/09540105.2011.652820>
- Choy KW, Zain ZM, Murugan DD, Giribabu N, Zamakshshari NH, Lim YM, et al. Effect of hydrolyzed bird's nest on β -cell function and insulin signaling in type 2 diabetic mice. *Front Pharmacol.* 2021;12:632169. DOI: <https://doi.org/10.3389/fphar.2021.632169>
- Murugan DD, Md Zain Z, Choy KW, Zamakshshari NH, Choong MJ, Lim YM, et al. Edible bird's nest protects against hyperglycemia-induced oxidative stress and endothelial dysfunction. *Front Pharmacol.* 2019;10:1624. DOI: <https://doi.org/10.3389/fphar.2019.01624>
- Careena S, Sani D, Tan SN, Lim CW, Hassan S, Norhafizah M, et al. Effect of edible bird's nest extract on lipopolysaccharide-induced impairment of learning and memory in Wistar rats. *Evid Based Complement Alternat Med.* 2018;2018:9318789. DOI: <https://doi.org/10.1155/2018/9318789>
- Yew MY, Koh RY, Chye SM, Othman L, Ng KY. Edible bird's nest ameliorates oxidative stress-induced apoptosis in SH-SY5Y human neuroblastoma cells. *BMC Complement Alternat Med.* 2014;14:391. DOI: <https://doi.org/10.1186/1472-6882-14-391>
- Sandech N, Jangchart R, Komolkriengkrai M, Boonyoung P, Khimmaktong W. Efficiency of Gymnema sylvestre-derived gymnemic acid on the restoration and improvement of brain vascular characteristics in diabetic rats. *Exp Ther Med.* 2021;22:1420. DOI: <https://doi.org/10.3892/etm.2021.10475>
- Yida Z, Imam MU, Ismail M, Ooi DJ, Sarega N, Azmi NH, et al. Edible bird's nest prevents high-fat diet-induced insulin resistance in rats. *J Diabetes Res.* 2015:760535. DOI: <https://doi.org/10.1155/2015/760535>
- Khalid M, Petroianu G, Adem A. Advanced glycation end products and diabetes mellitus: mechanisms and perspectives. *Biomolecules.* 2022;12(4):542. DOI: <https://doi.org/10.3390/biom12040542>
- Yamagishi S. Role of advanced glycation end products (AGEs) and receptor for AGEs (RAGE) in vascular damage in diabetes. *Exp Gerontol.* 2011;46(4):217-224. DOI: <https://doi.org/10.1016/j.exger.2010.11.007>
- Baelde HJ, Eikmans M, Lappin DWP, Doran PP, Hohenadel D, Brinkkoetter PT, et al. Reduction of VEGF-A and CTGF expression in diabetic nephropathy is associated with podocyte loss. *Kidney Int.* 2007;71:637-645. DOI: <https://doi.org/10.1038/sj.ki.5002068>
- Komolkriengkrai M, Jangchart R, Sandech N, Vongvatcharanon U, Khimmaktong W. Beneficial effects of gymnemic acid on three-dimensional vascular architecture and expression of vascular endothelial growth factor of intrarenal segmental and interlobar arteries in diabetic rat

- kidney. *Funct Foods Health Dis.* 2022;12(6):340. DOI: <https://doi.org/10.31989/ffhd.v12i6.940>
21. Qi MY, He YH, Cheng Y, Fang Q, Ma RY, Zhou SJ, et al. Icarin ameliorates streptozocin-induced diabetic nephropathy through suppressing the TLR4/NF-KB signal pathway. *Food Funct.* 2021;12:1241-1251. DOI: <https://doi.org/10.1039/D0FO03007A>
 22. Asadipooya K, Uy EM. Advanced glycation end products (AGEs), receptor for AGEs, diabetes, and bone: literature review. *J Endocr Soc.* 2019;3:1799-1818. DOI: <https://doi.org/10.1210/je.2019-00204>
 23. Tan KCB, Chow WS, Ai VHG, Metz C, Bucala R, Lam KSL. Advanced glycation end products and endothelial dysfunction in type 2 diabetes. *Diabetes Care.* 2002;25(6):1055-1059. DOI: <https://doi.org/10.2337/diacare.25.6.1055>
 24. Shimizu F, Sano Y, Haruki H, Kanda T. Advanced glycation end-products induce basement membrane hypertrophy in endoneurial microvessels and disrupt the blood-nerve barrier by stimulating the release of TGF- β and vascular endothelial growth factor (VEGF) by pericytes. *Diabetologia.* 2011;54:1517-1526. DOI: <https://doi.org/10.1007/s00125-011-2081-2>
 25. Grant DS, Kleinman HK. Regulation of capillary formation by laminin and other components of the extracellular matrix. *EXS.* 1997; 79:317-333. DOI: https://doi.org/10.1007/978-3-0348-8893-2_22
 26. Caligiuri G. CD31 as a therapeutic target in atherosclerosis. *Circ Res.* 2020;126(9):1178-1189. DOI: <https://doi.org/10.1161/CIRCRESAHA.120.315935>
 27. Krüger-Genge A, Blocki A, Franke RP, Jung F. Vascular endothelial cell biology: an update. *Int J Mol Sci.* 2019;20(18):4411. DOI: <https://doi.org/10.3390/ijms20184411>
 28. Sun D, Wu L, Lan S, Chi X, Wu Z. B-asarone induces viability and angiogenesis and suppresses apoptosis of human vascular endothelial cells after ischemic stroke by upregulating vascular endothelial growth factor A. *PeerJ.* 2024;12:e17534. DOI: <https://doi.org/10.7717/peerj.17534>
 29. Ban CR, Twigg SM. Fibrosis in diabetes complications: pathogenic mechanisms and circulating and urinary markers. *Vasc Health Risk Manag.* 2008; 4:575-586. DOI: <https://doi.org/10.2147/vhrm.s2824>
 30. Wolf G, Schneider A, Wenzel U, Helmchen U, Stahl RA. Regulation of glomerular TGF- β expression in the contralateral kidney of two-kidney, one-clip hypertensive rats. *J Am Soc Nephrol.* 1998;9(5):763-772. DOI: <https://doi.org/10.1681/ASN.V958763>
 31. Takahashi T, Harris RC. Role of endothelial nitric oxide synthase in diabetic nephropathy: lessons from diabetic eNOS knockout mice. *J Diabetes Res.* 2014;590541. DOI: <https://doi.org/10.1155/2014/590541>
 32. Mahdi A, Tengbom J, Alvarsson M, Wernly B, Zhou Z, Pernow J. Red blood cell peroxynitrite causes endothelial dysfunction in type 2 diabetes mellitus via arginase. *Cells.* 2020;9(7):1712. DOI: <https://doi.org/10.3390/cells9071712>
 33. Lin PS, Chang HH, Yeh CY, Chang MC, Chan CP, Kuo HY, et al. Transforming growth factor beta 1 increases collagen content and stimulates procollagen I and tissue inhibitor of metalloproteinase-1 production of dental pulp cells: role of MEK/ERK and activin receptor-like kinase-5/Smad signaling. *J Formos Med Assoc.* 2017; 116:351-358. DOI: <https://doi.org/10.1016/j.jfma.2016.04.008>
 34. Paunas FTI, Finne K, Leh S, Osman TAH, Marti HP, Berven F, et al. Characterization of glomerular extracellular matrix in IgA nephropathy by proteomic analysis of laser-captured microdissected glomeruli. *BMC Nephrol.* 2019;20(1):410. DOI: <https://doi.org/10.1186/s12882-019-1615-2>